

CHAPTER II

LITERATURE REVIEW

2.1 Piezoelectric Materials

2.1.1 Principle of Piezoelectric Material

Piezoelectricity is a Greek term of "Pressure Electricity" mean generation of electricity when applied mechanical signal (direct effect). Piezoelectric material also exhibited converse effect which response to electrical signal by change its shape or mechanically deform. This active material display a relationship between the elastic variables (X stress, X strain) and the dielectric variables (D electric displacement, E electric field) (Furukawa, 1989). The combination of these variables defined into 4 constants, piezoelectric strain constant d (C/N or m/V), piezoelectric voltage constant g (Vm/N or m²/C), stress constant e (C/m or N/Vm) and strain constant h (V/m or N/C) as shown in Figure 2.1 were given by:

$$d = \left(\frac{\partial D}{\partial X} \right)_E = \left(\frac{\partial x}{\partial E} \right)_X \quad g = \left(\frac{\partial E}{\partial X} \right)_D = - \left(\frac{\partial x}{\partial D} \right)_X$$

$$e = \left(\frac{\partial D}{\partial x} \right)_E = \left(\frac{\partial X}{\partial E} \right)_x \quad h = \left(\frac{\partial E}{\partial x} \right)_D = - \left(\frac{\partial X}{\partial D} \right)_x$$

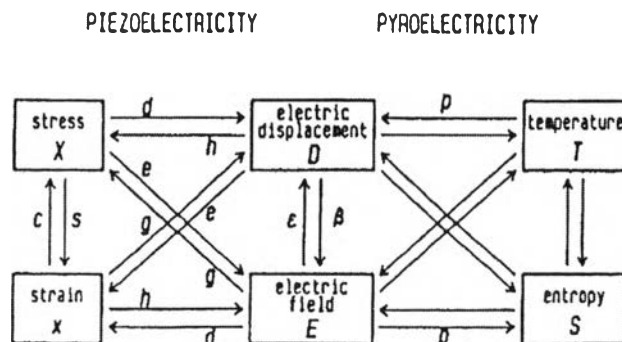


Figure 2.1 Definition of piezoelectric and pyroelectric constants.

The piezoelectric coefficient, d_{ij} , the first subscript is the direction of the electric field or charge displacement while the second subscript gives the direction of the mechanical deformation or stress. The C_2 crystallographic symmetry typical of synthetic oriented, poled polymer film leads to the cancellation of all but five of the d_{ij} components (d_{31} , d_{32} , d_{33} , d_{15} and d_{24}). For poled film, biaxially oriented or unoriented, the piezoelectric coefficient possesses to be equal, $d_{31} = d_{32}$ and $d_{15} = d_{24}$. Most natural biopolymers possess D symmetry which yields a matrix possessing only the shear piezoelectricity components d_{13} and d_{25} . Since the d_{33} constant is difficult to measure without constraining the sample in its lateral dimension, it is typically determined from Equation 2.1 which relates the constants to the hydrostatic piezoelectric constant, d_{3h} .

$$d_{3h} = d_{31} + d_{32} + d_{33} \quad (2.1)$$

2.1.2 Structural Requirement for Piezoelectric Polymer

Both of amorphous and semi-crystalline polymer require essential element as followed:

- The presence of permanent molecular dipole moment.
- The ability to orient the molecular dipoles.
- The ability to certain the orientation of molecular dipoles.
- The ability of material to undergo large strain when applied stress.

2.1.3 Piezoelectric Properties of Polymer

The piezoelectric properties of polymer are originated from aligned dipoles in uniaxial direction with a non-centrosymmetric crystal. The comparison between piezoelectric ceramic and polymer as shown in Table 2.1. The piezoelectric strain constant (d_{31}) of Lead Zirconium Titanate (PZT) is much higher than PVDF. However, polymer has much lower dielectric permittivity led to high piezoelectric stress constant ($g_{31} = 240 \text{ mV}\cdot\text{m}/\text{N}$). Mean that polymers are better in sensor applications than ceramics. Moreover, polymer offer attractive properties like lightweight, tough, easy of process and flexibility.

Table 2.1 Properties comparison of common piezoelectric polymer and ceramic

<i>Materials</i>	<i>d₃₁ (pm/V)</i>	<i>g₃₁ (mV-M/N)</i>	<i>k₃₁</i>
PVDF	28	240	0.12
PZT	175	11	0.34

In last decades, the development of piezoelectric polymer have been growing rapidly, poly(vinylidene fluoride) (PVDF) and its copolymers with trifluoroethylene (TrFE) and tetrafluoroethylene (TFE) become commercially available piezoelectric polymers since they display higher piezoelectric coefficient compare to other polymers. Odd numbered nylons, the next most widely investigated semicrystalline piezoelectric polymers, have excellent piezoelectric properties at elevated temperatures but have not yet been embraced in practical application. Other semi-crystalline polymers including polyureas, liquid crystalline polymers, biopolymers and an array of blend combinations have been studied for their piezoelectric potential. The Table 2.2 shows piezoelectric constants for several semi-crystalline polymers and biopolymer.

Table 2.2 Piezoelectric properties of polymers

<i>Polymer</i>	<i>d₃₁ (pC/N)</i>
Synthetic polymer	
PVC	5
PTrFE	12
Nylon-7	17
PVDF	20-28
Bio-polymer	
Cellulose	0.15
Wool	0.1
Poly-lactic acid	10
Poly-β-hydroxybutyrate	1.3

Table 2.3 Comparison between the different methods for enhancing the dielectric permittivity

	Type of fillers	Advantages	Drawbacks
Random composite	Dielectric	- High dielectric permittivity	- large percentage of filler - increase in elastic modulus
	Conductive	- High dielectric permittivity for low percentage of filler	- increase in conductivity - decrease of maximum voltage possible to apply
Polymer Blend	No fillers	- Very high dielectric permittivity - No problem of conductivity - No mechanical reinforcement	- complication of process

The piezoelectric properties of materials are strongly depend on dielectric properties. Many research studied to enhance dielectric behavior of materials which there are various methods available for enhancing the dielectric permittivity of polymers are listed in Table 2.3 . The advantages and drawbacks of each technique are also shown the table.

2.2 Poly(vinylidene fluoride)

Poly(vinylidene fluoride) (PVDF) or poly-1,1-difluoroethane, is a semi-crystalline polymer consisting of $-\text{CH}_2\text{CF}_2-$ repeating unit (A. Salimi, 2003,). The common polymorphs of PVDF referred to α and β polymorphs (M. El Achaby,2012). The α -phase has Trans–Gauche–Trans–Gauche (TGTG) conformation with in monoclinic unit cell resulting in non piezoelectric behavior which was generated during crystallization from melting process. The β -phase of PVDF, an orthorhombic unit cell with all Trans conformations (TTTT) as shown Figure 2.2 , is an active phase explored highest net dipole moment resulting in good piezoelectric and pyroelectric properties.

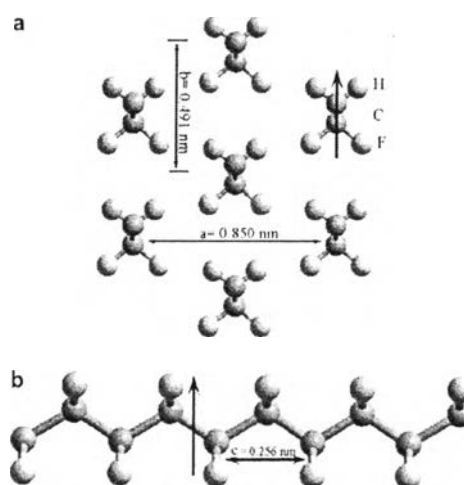


Figure 2.2 Beta-phase structure of PVDF with orthorhombic unit cell. (G. Zhu et al. 2008)

Since PVDF in polar β -phase form is well-known in electrically active polymer which has been introduced in sensors, transducers, and actuators for various applications such as robotics, acoustics and ultrasound. This piezoelectric β -phase can be achieved from other polymorphic phases by different techniques. Mechanical stretching (Figure 2.3) is one of important techniques to induce crystalline phase transformation (α - to β -phase). Stretching polymer at a given temperature is a

essential step to align amorphous regions stand in the film plane then applied an strong electric field across the film thickness to fixed the crystalline orientation and align molecular dipole in the same direction as applied electric field.

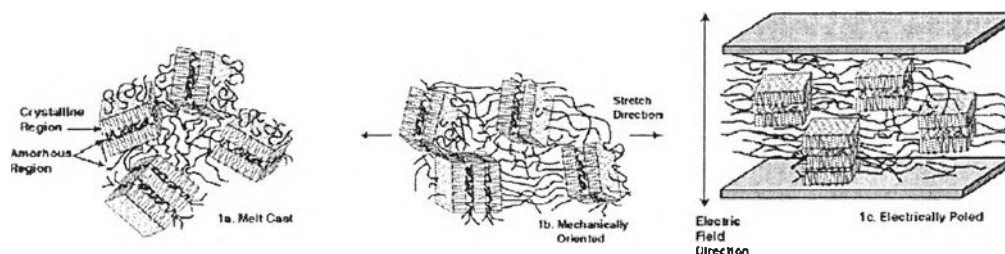


Figure 2.3 Stretching and electrical poling to induced β -phase of PVDF.

The other techniques were used to obtain β polymorph such as poling under a large electric field, thermal annealing and electrospinning (one steps of solution casting and poling) (Hong-Feng Guo, 2012). Up to present, the addition of nucleating agent such as clays, organoclays, modified graphene and carbon nanotubes, has drawn attention to allow phase transformation of PVDF to its β -phase via melt casting.

The ferroelectricity in PVDF was defined as hysteresis loop of polarization, P , and applied electric field, E , as shown in Figure 2.4. The present of a spontaneous polarization, P_s , together with polarization reversal in PVDF can be proof of ferroelectric material. Besides, the coercive field, E_c , and remanent polarization, P_r were found in P - E hysteresis loop, which are essential properties to study ferroelectric behavior. The E_c is the point where the hysteresis intersects with the horizontal axis. The P_r corresponds to the point where the loop intersects with the vertical axis. The values of E_c and P_r are dependent on the temperature and frequency of measurement.

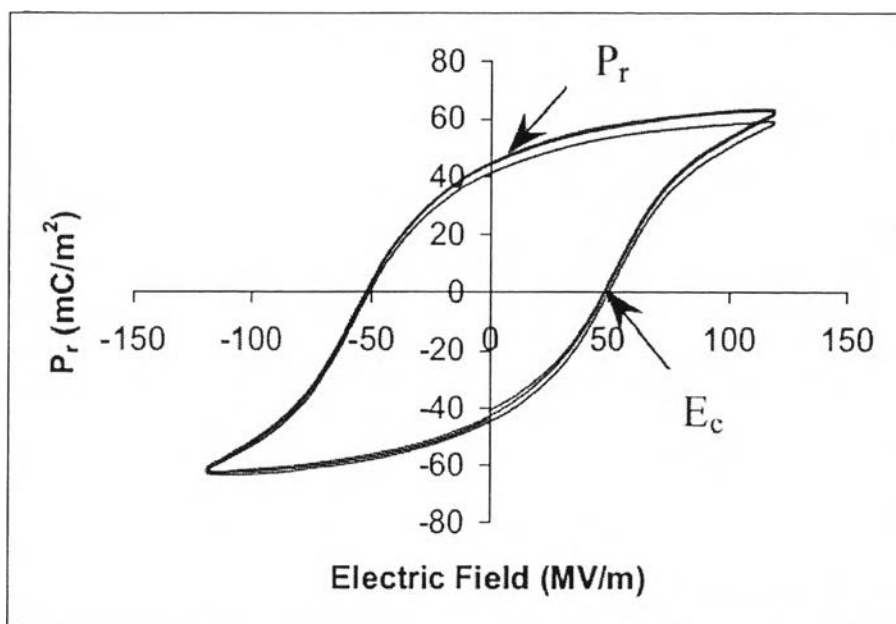


Figure 2.4 P-E hysteresis loop for PVDF.

2.3 Cellulose

2.3.1 Source of Cellulose

Cellulose, one of the most common abundant and renewable polymer on the earth, is well-known commercial biopolymer. Cellulose has an unique properties due to their biodegradability, light weight, transparency, and high strength (Bledaki and Gassan, 1999). In 1839, French chemist Anselme Payen is first isolated cellulose from plant matter. He reported that cellulose has an identical structure as starch, but it exhibited the difference in structure and properties. However, cellulose from natural resource including agricultural industries is mostly composing of lignin and hemicellulose in the cell wall of plants (Bhatnager and Sain, 2005). In order to use purified cellulose, it needs isolation and purification steps to remove impurities out which composition of cellulose varies according to source. The statistical average of chemical composition of cellulose natural sources is shown in Table 2.4.

From the fundamental point of view, plant-based celluloses have some impurities resulting in the difficulty to modify via chemical reaction. On the other hand, some of researchers have proposed the novel method of cellulose preparation from bacterial species which called bacterial cellulose. This cellulose prepared from bacterial also exhibits the excellent properties as well as plant-based cellulose. Moreover, the uniformity of cellulose prepared from bacterial is easier to control by means of bacterial digestion mechanism. This concept consequently leads to enhance the performance of this materials if it will be used in relevant applications

From the fundamental point of view, plant-based celluloses have some impurities resulting in the difficulty to modify via chemical reaction. On the other hand, some of researchers have proposed the novel method of cellulose preparation from bacterial species which called bacterial cellulose. This cellulose prepared from bacterial also exhibits the excellent properties as well as plant-based cellulose. Moreover, the uniformity of cellulose prepared from bacterial is easier to control by means of bacterial digestion mechanism. This concept consequently leads to enhance the performance of this materials if it will be used in relevant applications.

Table 2.4 Chemical composition of some cellulose sources (Heinze and Liebert, 2001)

Source	Composition (%)			
	Cellulose	Hemicellulose	Lignin	Extract
Wheat straw	30	50	15	5
Bagasse	40	30	20	10
Softwood	40-44	25-29	25-31	1-5
Hardwood	43-47	25-35	16-24	2-8
Flax (retted)	71.2	20.6	2.2	6.0
Jute	71.5	13.6	13.1	1.8
Ramie	76.2	16.7	0.7	6.4
Cotton	95	2	0.9	0.4

2.3.2 Chemical Structure of Cellulose

The structure of cellulose is linear homopolymer composed of D-glucopyranose units (also called anhydroglucose unit, AGU) linked by β -1,4-glycosidic linkage at C₁ and C₄ carbon position as shown in Figure 2.5 (Jonas and Farah, 1997, Heinze and Liebert, 2001).

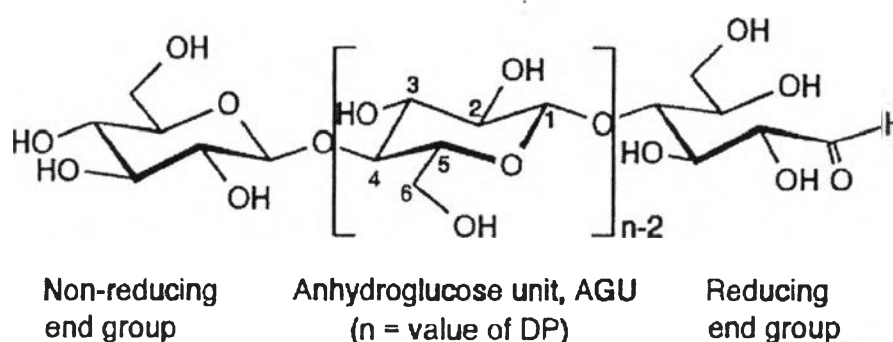


Figure 2.5 Molecular structure of cellulose.

In general, cellulose chain is fully extended form. Their repeating unit is rotated at an angle of 180° with respect to adjacent molecule. Cellulose chain has two different chain ends, one chain end has free α - or β -hydroxyl group at C_1 position act as reducing group while the other one no reducing end group. The length of cellulose chains depend on degree of polymerization (DP). The DP can vary from about 20 in case of lab production to about 7000 in cotton or more than 10000 in bacterial cellulose.

In term of chemical structure, the repeating unit of cellulose consists of three reactive hydroxyl groups at the C_2 and C_3 (secondary hydroxyl group) and C_6 carbon atoms, resulting in strong both intra- and intermolecular hydrogen bonding (Figure 2.6). This excellent concept can be further led to have high degree of crystallinity, high oriented, and three-dimensional crystal structures. These hydrogen bonds make cellulose difficult to dissolve in any common organic solvents and disperse in melted polymer via thermal process. In contrast, these reactive hydroxyl groups can undergo various chemical reactions such as esterification, etherification prior to use in any applications.

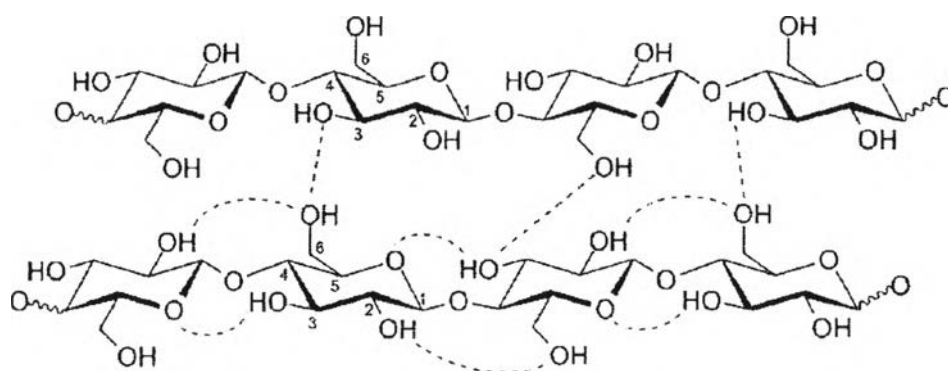


Figure 2.6 Intra- and intermolecular hydrogen bonding of cellulose chain.

On the other hand, the use of cellulose is mainly concerned on solid form. We therefore have to consider on this. Solid cellulose can typically form a microcrystalline structure with regions of high order, i.e. crystalline regions, and regions of low order, i.e. amorphous regions. Naturally occurring cellulose crystallizes in monoclinic sphenodic structures (Bledzki and Gassan, 1999) can be seen in Figure 2.7. The molecular chains are well oriented in fiber direction.

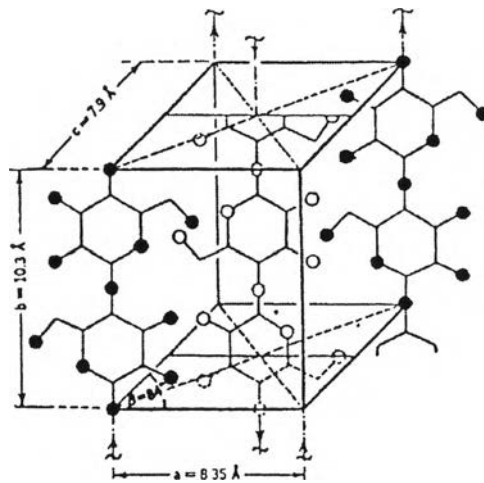


Figure 2.7 Monoclinic sphenoidal structure of cellulose.

Although cellulose constitutes a significant portion of material, mechanical properties such as tensile strength and stiffness of the plain material are inferior to the properties of neat cellulose. Figure 2.7 shows natural fibers that obtain from different processes have different mechanical properties (Young's modulus). The Young's modulus of cellulose crystallites give up to 250 MPa which about 25 times of wood.

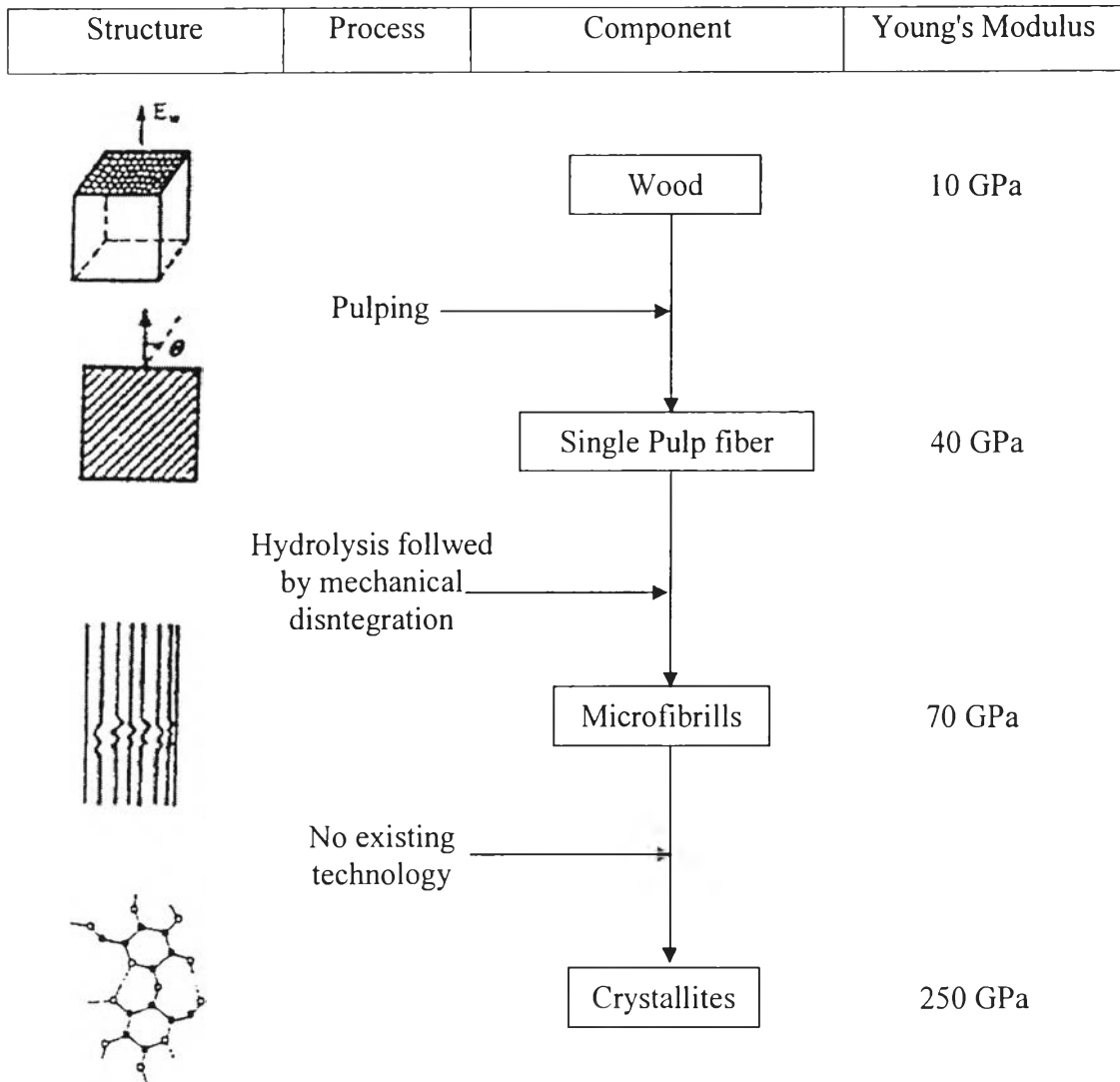


Figure 2.8 Correlation between structure, process, component and Young's modulus.

2.3.3 Bacterial Cellulose

Bacterial cellulose (BC), an alternative cellulosic source, has chemically structure as same as plant cellulose, which is anhydroglucose units bonded together via β -1,4-glycosidic linkage as shown in Figure 2.6. The Table 2.5 shows classification of bacteria's capability to produce cellulose. Even there are a number of bacteria species were reported capable of producing bacterial cellulose but only bacteria named *Acetobacter xylinum* is the most efficient producer (El-Saied, 2004 and Bae and Shoda, 2004), which produced cellulose in ribbon-shaped like. The BC that produced by *A. Xylinum* has superior properties including a highly pure source of cellulose, high crystallinity, hydrophilicity, high tensile strength and and ultra-fine fiber network structure

Table 2.5 A classification of the bacteria's capability to produce cellulose

<i>Genus</i>	<i>Cellulose Structure</i>
Acetobacter	pellicle composed of ribbons
Achromobacter	fibrils
Aerobacter	fibrils
Agrobacterium	short fibrils
Alicalingenes	fibrils
Pseudomonas	no distinct fibrils
Rhizobium	short fibrils
Sarcina	amorphous cellulose
Zoogloea	not well defined

Bacterial cellulose has been substantially utilized in food industry (Gindl and Keckes, 2005). An example is nata de coco, a coconut gel dessert prepared by bacterial fermentation of coconut water immersed in sugar sirup. Though originally the Filipino dessert, it becomes very popular as diet food in Japan. Also, owing to its good liquid adsorption, ability to withstand sterilisation and non-allergenic properties, bacterial cellulose is extensively employed in many medical applications. The examples are artificial skin, blood vessels and ureters (Ciechanska, 2004). Bacterial cellulose is also applied as a binder in the paper industry to improve

the strength as well as the durability of paper. Other uses includes diaphragms in audio components. Among various applications, BC has drawn scientific interest as seen in the statistics of publications shown in Figure 2.9. which rapidly increase in the past decade.

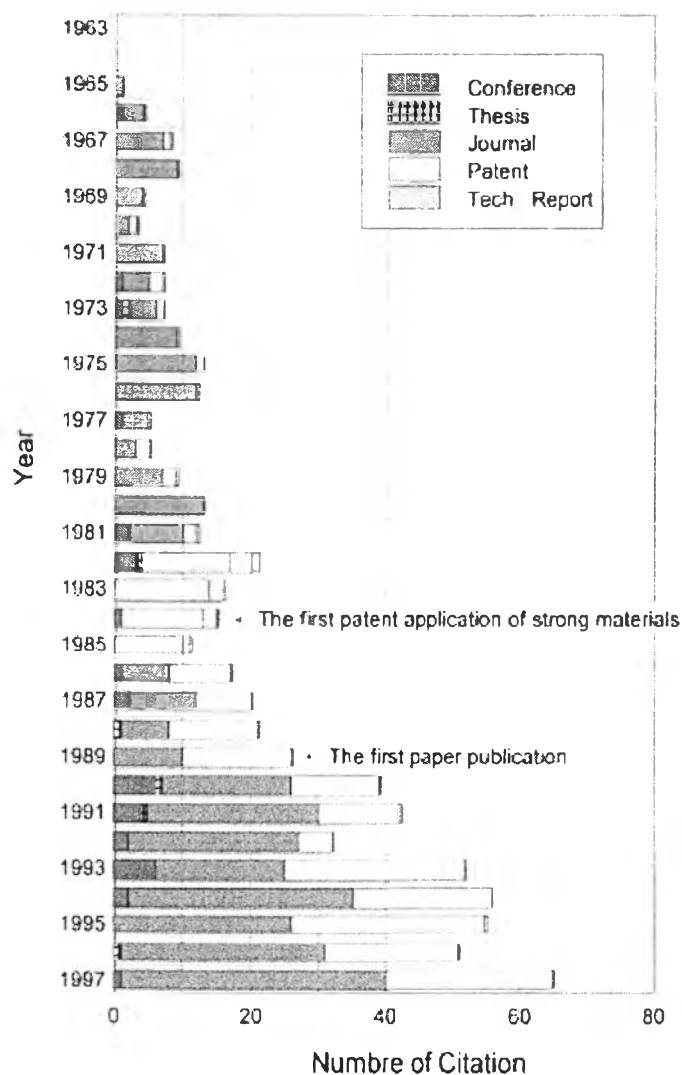


Figure 2.9 Statistics publication of bacterial cellulose related articles. (IGUCHI et, al, 2004)

2.3.3.1 Properties of bacterial cellulose

Bacterial cellulose synthesised by *Acetobacter xylinum* has been extensively investigated by Czaja *et al.* (2004) (strain NQ-5) and Watanabe *et al.* (1998) (strain BPR2001). Some of the reported properties are listed in Table 2.6. An air-dried bacterial cellulose sheet has tensile strength of 256 MPa with the Young's modulus of 17 GPa (Iguchi *et al.*, 2000). The elastic modulus of bacterial cellulose single fibril was recently measured using atomic force microscopy (AFM) by Guhados *et al.* (2005) to be 78 GPa, which is comparable to glass fibre. The elastic modulus of the bacterial cellulose single fibril was also estimated using a Raman spectroscopic technique to be 114 GPa by Hsieh (2008). This modulus was predicted from a calibration of the Raman band shift against the elastic modulus. In comparison, the elastic modulus of the crystalline cellulose (Cellulose-I) was measured by X-ray Diffraction (XRD) to be 138 GPa as reported by Nishino *et al.* (2004).

Table 2.6 Properties of bacterial cellulose

Features	Watanabe <i>et al.</i> (1998)		Czaja <i>et al.</i> (2004)	
	Agitated Culture	Static Culture	Agitated Culture	Static Culture
Crystallinity index (%)	63	71	-	-
Crystallite size (nm)	6.9	7.4	6.4-7.9	6.7-8.6
Crystallinity (%)	72	80	84	89
Cellulose I (%)	61	73	71	76
Degree of polymerization	10900	14400	-	-
Water holding capacity (g water/g cellulose)	170	45	-	-

2.3.4 Development Cellulose Electro-active paper

An electromechanical coupling effect in woods were firstly discovered by Bazhenov (1950). In 1955, Fukada demonstrated that the shear piezoelectricity of cellulose arise from the uniaxial oriented cellulose crystallites and their monoclinic structure. The shear piezoelectric is observed by measured electrical polarization perpendicular to the applied stress direction. The piezoelectric modulus of cellulose are strongly depend on an angle between applied pressure and fiber direction (observed by rotated specimen) as shown in Figure 2.10. The obtained piezoelectric modulus d_{14} is about -2.6 which much less than d_{11} modulus of quartz (~ 65).

The internal rotation of polar groups that associated with asymmetric carbon atoms of cellulose exhibited shear piezoelectricity are well-known. However, the used of cellulose as a smart material which sense to external stimuli like electrical and mechanical has not been explored. Until Kim and Yun (2006) demonstrated the potential of cellulose electro-active paper can be use in various applications such as biomedical devices, sensors, actuators, micro-electromechanical systems and flexible electrical displays. It offer many advantages in term of biocompatible, light weight low cost, and large deformation.

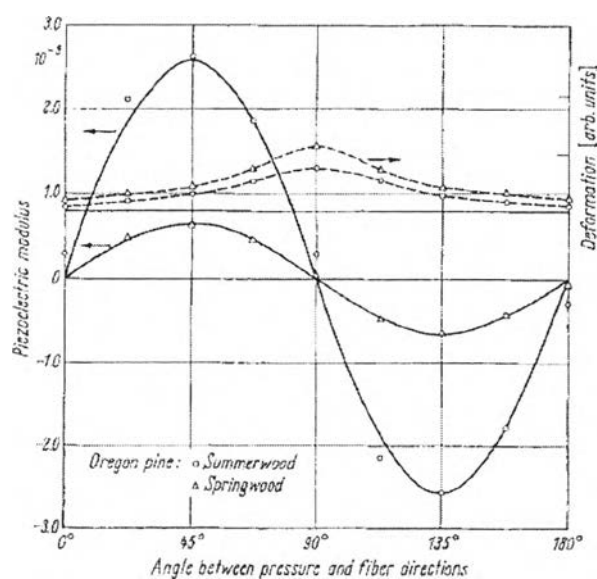


Figure 2.10 Piezoelectric modulus vs. angle between pressure direction and fiber direction for Oregon pine.

In 2007 (Kim *et al.*) studied in-plane piezoelectric charge constant d_{31} of regenerated cellulose which quantified by quasi-static relation between induced charge on electrode area and applied in-plane stress. the orientations of cellulose film (Figure 2.11) 0° , 45° and 90° , resulting in different d_{31} which are 8.01, 28.2, and 23.4 pC/N, respectively.

As monoclinic crystalline structure of cellulose display piezoelectric effect, the piezoelectricity of cellulose derivatives such as cellophane, celluloid, and viscose rayon have been reported which depending on fiber orientation and degree of crystallinity. The regenerated nanocrystalline cellulose which their crystallite in cellulose II generated large piezoelectricity about 35-60 pC/N. Csoka and co-workers studied the shear piezoelectric effect (d_{25}) of cellulose nanocrystal in native crystalline structure. The degree of alignment of nanocellulose thin film as high as 88% yield to highest d_{25} as high as 2.1 Å/V.

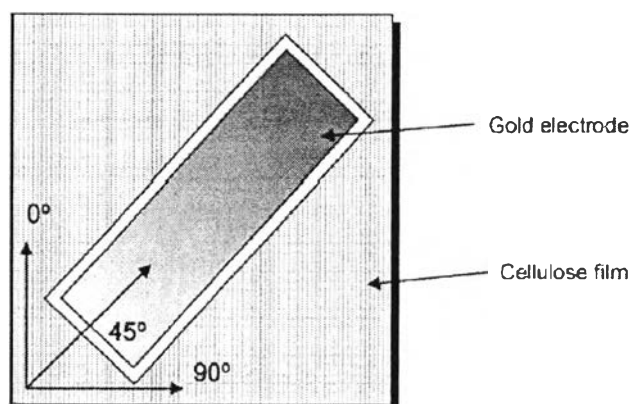


Figure 2.11 The orientation of cellulose film.

Yun, S. and Kim, J (2010) studied piezoelectric behavior in the presence of covalent grafting of multi-walled carbon nanotube (MCNT) on hydroxyl group of cellulose. The alignment of MCNT in composites are induced by mechanical stretching at different stretching ratios (S_R), 1.0, 1.4, 1.6, 1.8. The increasing on degree of alignment of composite resulting in increase piezoelectric constant, Young's modulus and also reduced electrical resistance. The piezoelectric properties of samples were measured by TSC measurement, the highest d_{31} was obtained from

composite with 45° orientation and applied S_R 1.8, the value as high as 72.0 ± 1.4 pC/N. Moreover, the depolarized current of composite is linearly increased with increasing poling electric field ranging from 500KV/m to 1.5 MV/m. as shown in Figure 2.12.

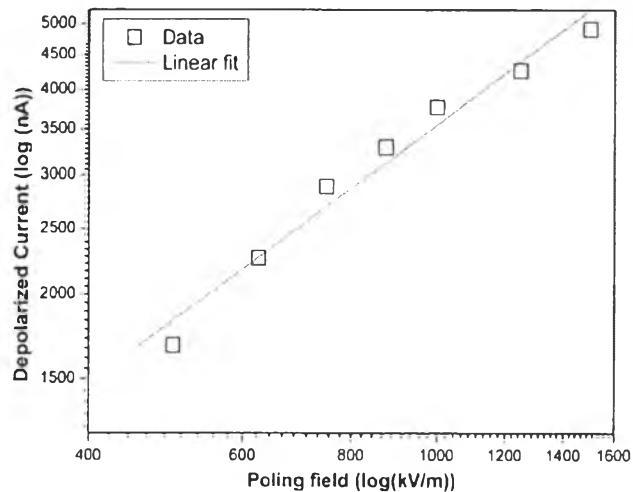


Figure 2.12 The depolarized current of aligned cellulose composite at various applied poling electric field by TSC measurement.